International Journal of Integrated Engineering: Special Issue 2018: Center for Graduate Studies, Vol. 10 No. 3 (2018) p. 63-68

DOI: https://doi.org/10.30880/ijie.2018.10.03.011

Influence of Friction Stir Process on Microstructure and Tensile Properties of LM28 Hypereutectic Al-Si Alloy

Samir Sani Abdulmalik*, Rosli Ahmad

Department of Manufacturing and Industrial Engineering, Universiti Tun Hussein Onn Malaysia, Johor, 86400, MALAYSIA

Received 7 January 2018; accepted 23 January 2018, available online 3 July 2018

Abstract: This paper reports an investigation of the influence of friction stir processing (FSP) on the microstructure modification, tensile properties and hardness of as cast hypereutectic LM28 aluminium silicon (Al-Si) alloy, aimed to decrease Silicon particles size, porosity, and enhancing tensile properties. Intense plastic deformation foisted by FSP resulted in a remarkable breaking up of the coarse eutectic and primary silicon particles into smaller ones, and closure of porosity. The area sizes of the fragmented Si particles decreased from 155.1 μm² to around 49.4 μm², aspect ratio of about 2.86 in the as cast condition decreased to around 1.63 after FSP. Porosity was also drastically reduced from 94 μm ECD, in the as cast condition to as low as 7.1 μm ECD. The strength and ductility of the alloy increased simultaneously after FSP. The increase in the tensile strength and ductility values after FSP, as compare to the as cast alloy was around 1.56, and 4.38 times respectively. The LM28 FS-processed alloy displayed an increase in quality index of around 1.97 times higher, than that of the as-cast alloy. The hardness of the alloy increased from 64.6 HV for the as-cast alloy to about 85.74 HV after FSP. Enhancement in all the properties was largely related to the pronounced changes of the shape, area size and distribution of the silicon particles along with the reduction of porosity FSP.

Keywords: Friction stir processing, hypereutectic cast alloy, microstructure, tensile properties

1. Introduction

Aluminium-silicon (Al-Si) cast alloys are used widely because of the many advantages they offer such as good castability, high strength, good weldability, wear and corrosion resistance [1]. Application of these alloys includes automotive engine blocks, cylinders heads, gear boxes, crank case and break cylinder [2]. The microstructure of these alloys particularly the hypereutectic series, consist of hard silicon particles distributed in ductile and soft aluminium matrix and hence, it is considered as in situ composite material. The major drawback of this material is the present of microstructural defects, like; porosities and large coarser silicon particles, which renders the alloy brittle accompany with low toughness, and low strength [3]. Strength can be improved by eliminating porosities and breaking the large silicon particles to smaller finer particles.

Several approaches such as alloying element addition and heat treatment have been used to improve the Al-Si alloy strengths by reducing the microstructural defects and improving the microstructure via changing the silicon particles morphology [4]. However, those approaches cannot effectively changed, redistribute the silicon particle uniformly, and eliminate the porosities [5]. A new microstructure modification method; friction stir processing FSP, was used in this study to improve the properties of Al-18Si-0.9Cu-1.15Ni Al-Si alloy. FSP is a variant of friction stir welding FSW. It selectively modify the microstructure in specific areas purposely to enhancing local mechanical properties [2, 6]. During FSP a rotating non-consumable tool having a shoulder and pin is plunged into a piece work material. The tool rubs against the work material and traverses, generates sufficient frictional heat. The heat coupled with intense plastic deformation by the tool pin stirring action and pressure due to the shoulder, result in fine grained, recrystallized microstructure [4]. FSP has been used in Al-Si alloys to improved mechanical properties, and shown remarkable improved properties and microstructure refinement [7-9]. It was reported that FSP effectively eliminates porosities, refines the coarser large primary silicon particles, and eutectic silicon by breaking up and distributing them into the aluminium matrix [6, 10].

Numbers of studies conducted on the effect of FSP were on the properties of hypoeutectic and eutectic Al-Si alloys [4, 7, 10], only limited studies were conducted to evaluate such properties of hypereutectic Al-Si alloys [5]. Furthermore, in both condition of hypoeutectic and hypereutectic alloy, the influence of FSP on the mechanical properties and microstructure still needs further studies, to understand more on the correlation between FSP parameters, mechanical and microstructure properties. Therefore, the aim of this work is to apply FSP, to modify the surface of Al-18Si-0.9Cu-1.15Ni

*Corresponding author: hd110194@siswa.uthm.edu.my

hypereutectic Al-Si alloy. The effect of tool rotation speeds and traverse speed on tensile properties and microstructure were investigated.

2. Materials and methods

The as received commercial cast hypereutectic Al-Si alloy LM28 ingot, were machined to 150 mm × 30 mm × 7 mm rectangular plates. The alloy has chemical composition: 18Si, 0.9Cu, 1.15Ni, 0.2Mn, 0.19Fe, 0.16Mg, 0.06Zn, and 79.34Al (in wt. %). As shown in Fig. 1, the surface of the plates were subjected to one pass friction stir processing using a non-consumable H13 tool steel, that has a cylindrical pin, the tool shoulder diameter was 17 mm; the length and diameter of the pin are 3.5 mm and 5 mm respectively. Vertical milling machine was employed for the FSP experiment using tool spindle rates of 800 rpm, 1000 rpm, 1200 rpm, and 1400 rpm, at a transverse rate of 22mm/min. Tool down force was held unchanged and tool angle set to 3˚ during the FSP experiments.

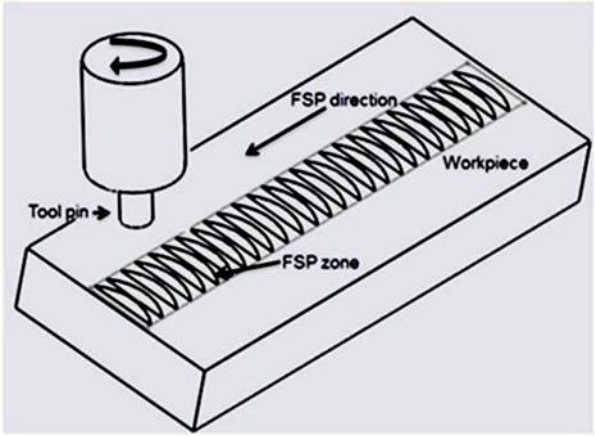

Fig. 1 FSP layout showing the FSP tool shape, and the resulting processed zone.

After FSP the FS-processed zones microstructures were investigated. The FSP treated samples were cut in the transverse direction, ground using different grades of sand paper, polished with 0.5 µm alumina paste, and etched, using 0.5 M hydrofluoric acid to reveal the microstructures. The samples microstructure examinations were accomplished using both optical microscope and scanning electron microscope (SEM). Image analysis technique was utilized for determining the sizes of the silicon particles, and porosity. To determine the tensile properties, tensile specimens were prepared from the samples (FS-processed regions) along the FSP direction as per ASTM: E8/E8M-11 Fig. 2, with the gauge length and gauge width of 25mm and 4mm respectively. The tensile test was carried out using a computer controlled Gotech universal testing machine at 1mm/min cross head speed. Tensile test is completed on both the as cast alloy and the FS-processed samples. At every condition, two specimens were tested and their average value was computed. Fracture surfaces of the tensile specimens were examined using SEM. Sample for microhardness test were grinded and polished. Vickers microhardness was measured across the samples processed zone, using a load of 500 g and dwell time of 10 s.

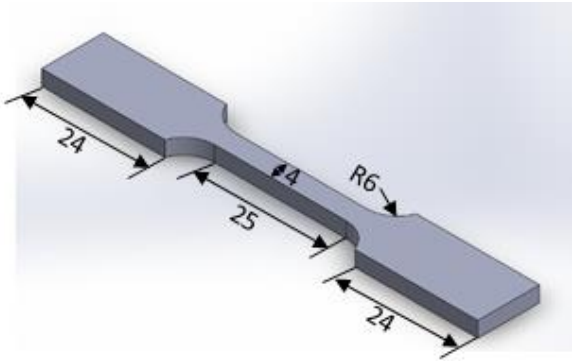

Fig. 2 The tensile specimen with its dimension in mm.
.

3. Results and Discussion

During FSP, due to the heat generated by the friction and stirring action, the material flows around the tool pin. FSP stir zones are prone to defects like cavity, tunnel, pin hole etc. due to excess or in sufficient heat input in the stir region [1]. The macrographs of the traverse cross section of hypereutectic LM28 alloy FS-processed samples for four different of rotational speeds, and a traverse speed are displayed in Table 1. Of the four tool rotation speeds used in processing the samples, defect free stir zone is produced at rotational speed of 1000rpm.

Table 1 Macrographs of the traverse cross-section of hypereutectic LM28 alloy specimens after FSP.

S/No.	Tool spindle speed (rpm)	Tool travel speed (mm/min)	Macrostructure AS RS
1	800	22	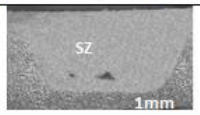
2	1000	22	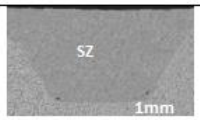
3	1200	22	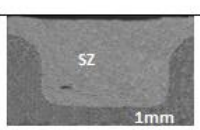
4	1400	22	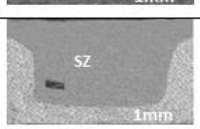

Figure 3(a) shows the micrographs of hypereutectic LM28 alloy. The base alloy consists of coarse needle-like

and platelet eutectic, and coarse primary silicon morphology, porosity. The distribution of the eutectic and the primary silicon was not uniform all through the aluminium matrix. Mean area of the eutectic and primary silicon was measured by an image analysis, and it was about 155.1 µm² with aspect ratio of 2.86. Moreover, porosity of up to ~94 equivalent circular diameter (ECD) µm was detected in the alloy. Fig. 3(b-e) presents optical micrographs of the LM28 alloy samples from the center of the stirred zones after FSP with varying rotation speeds. The micrographs clearly display the significant influence of FSP on the shape and size of silicon particles.

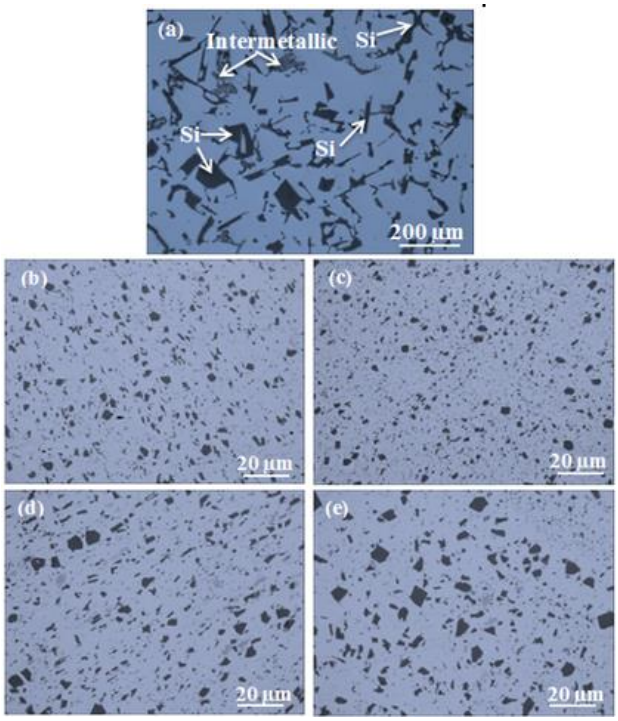

Fig. 3 Optical micrograph from the center of stirred zone of LM28 alloy after single pass FSP using 22 mm/min at (a) base alloy, (b) 800 rpm, (c) 1000 rpm, (d) 1200 rpm, (e) 1400 rpm.

Quantitative measurements of the silicon particles sizes, and aspect ratio, of the as FS-processed LM28 samples, relative to tool transverse speeds 22mm/min and tool rotational speeds 800 rpm, 1000 rpm, 1200 rpm, and 1400 rpm, is plotted in Fig. 4. FSP resulted in considerable breaking down of the coarse eutectic and coarse primary silicon particles, and forming a better distribution of finer and near circular silicon particles in the aluminium matrix. Such microstructure transformation is been reported in other Al-Si alloy [10]. The mean particle area and aspect ratio were measured to be 52.0 µm² /1.80, 49.4 µm² /1.63, 61.96 µm² /1.87 and 72.47 µm² /1.95, for tool rotation rates of 800 rpm, 1000 rpm, 1200 rpm and 1400 rpm, respectively. As the rotation speed increases the particles appears to show an increase in the average particle area size and aspect ratio. This observation agreed with the results presented by previous researcher [6]. Nevertheless, the particles sizes achieved in this investigation are very much smaller compare to that of the cast alloy 155 µm² /2.86 before FSP. Demonstrating that FSP led to about three times reduction in particle size and shape in terms of mean area values. Also notable were the lower aspect ratio values associated with the FSP microstructure. Earlier studies have demonstrated that on friction stir processing Al-Si eutectic completely recrystallizes and finer recrystallized grain structure is achieved. Severe plastic deformation and material flow caused by the stirring action of the pin and the high heat to which the material is exposed during FSP because of the frictional heat, are responsible for the grain refinement and dynamic recrystallization present [2, 11]. FSP also results in the closure of casting porosity and a homogenized microstructure. This could convert the as-cast material into a near-wrought condition, this homogenized and refined microstructure along with the closure of porosity results in improved mechanical properties [1, 12].

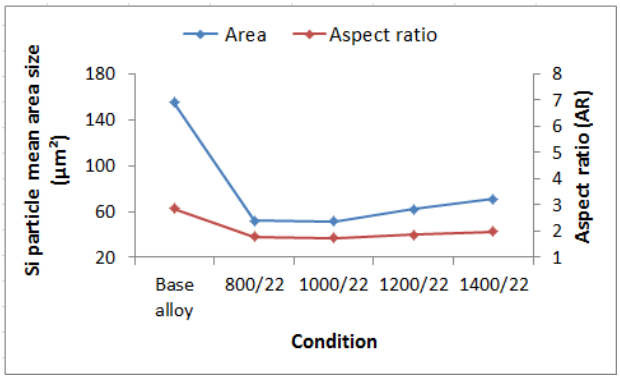

Fig. 4 Mean silicon particles sizes, and aspect ratio of base alloy and FS-processed LM28 samples, at 22 mm/min traverse speed and various tool rotational speeds.

Porosity has been significantly decreased from 94 µm ECD, in the as cast condition to as low as 7.1 µm ECD after FSP: Fig. 5 due to plastic deformation of the material under the high downward force and shear forces of the tool [13]. This trend is consistence with finding of Guru et al., influence of FSP on aluminium silicon LM25 cast alloy [9]. Elimination of porosity significantly assisted in improving the mechanical properties [5].

It was observed that for all the combination of rotational and traverse tool speeds used in this investigation, FSP induced considerable effect on the microstructure of the base alloy, due to the stirring action of the tool at plastic condition [1]. In Fig. 4 and Fig. 5, the silicon particles sizes and porosity decreases as rotation speed increase from 800 rpm to 1000 rpm, due to intense stirring action. However, increasing the tool rotation speed beyond 1000 rpm does not result to further decrease. The high heating at higher tool rotation speeds softens the material around the pin. Then, the breakdown of the particles would not be further intensify, because it became easy for the particles to flow with the plastic flow of the matrix [7, 14]. The observed variation of Si

particles and porosity at different tool speeds may be connected to difference in frictional heat produced and stirring effect at those processing condition [7].

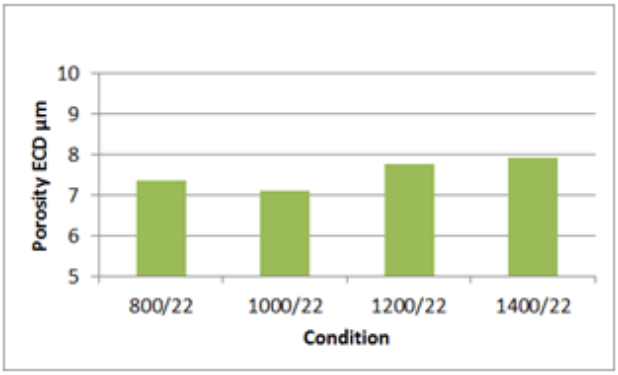

Fig. 5 Porosity at the center of SZ after FSP.

Figure 6 shows variation of tensile properties and quality index of the base alloy before and after FSP at a various tool rotational speeds and fixed traverse speed. As-cast base alloy shows a typical brittle material with low elongation. However after FSP, it was transformed to a ductile material. Evidently, FSP improved the ductility and strength of the alloy simultaneously, similar pattern was reported by [15]. The average values of the strengths and ductility obtained presented. In Fig. 6, it is visible to observe that before FSP the mean tensile strength (UTS), of the base alloy: 118 MPa, mean elongation to failure (%El): 1.7 %, and mean (Q): 156 MPa, ware lower compared to all the FS-processed samples. That was largely because of the presence of porosities and larger brittle silicon particles, presence in the alloy and acted as crack initiation sites [16].

After FSP the FS-processed samples showed significant increases in tensile properties. The ultimate tensile strength (UTS) is improved up to 184 MPa. The ductility of 7.47 % meanwhile is largely due to the refinement of the microstructure and the reduction/elimination of porosities. Other studies also have found that the tensile properties and fatigue of cast aluminium silicon alloys improved with refined microstructure, and reducing casting defect such as porosities size and density [9, 17, 18]. Sample processed at 1000 rpm shows higher tensile strength and elongation 184MPa / 7.47 % compared with the other samples. The increase in rotation speed above the 1000 rpm generates cavity defect in the retreating side of 1200 rpm, 1400 rpm samples (Table 1), due to abnormal stirring. The turbulence of softened metal is not consolidated in the retreating side of the samples. Similar phenomenon was reported by Jayaraman et al., for the rotation speed of higher than 900 rpm [1]. The higher tensile strength, elongation obtain at the 1000 rpm is related to the uniform distribution of small, fine silicon particles in the aluminium matrix of the stir zone Fig. 3(c), which mean at that condition there was sufficient stirring and proper consolidation of material and plasticization [19]. Whereas the reduction of the strength at 1200 rpm (183 MPa / 5.78 %) to 1400 rpm (158 MPa / 5.26 %) is due to the coarse/increased primary/eutectic Si particles in the matrix [6].

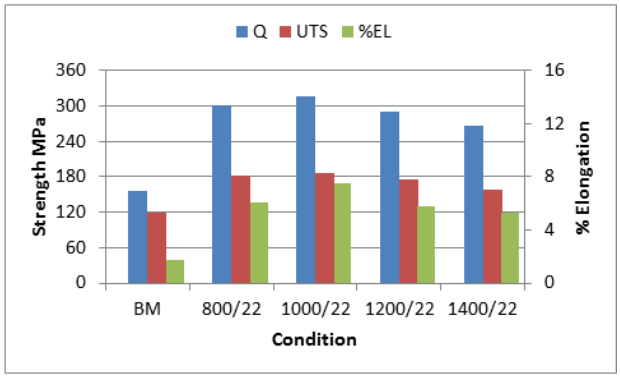

Fig. 6 Variation of tensile properties and quality index for as cast base metal, and after FSP at various tool rotation speeds.

A significant heat rise leads to particles coarsening, this in turn can cause a decrease in strength [2, 20]. The effect of the FSP on the performance of the LM28 alloy was evaluated using a numerical index that depends on the metallurgical qualities of the alloy: quality index (Q) [13]. Rather than tensile and elongation alone, the quality index combines the strength and ductility and presents a description of the true tensile properties of the cast material and samples [21]. The as cast alloys quality index was increased to 300.8 MPa, 315.4 MPa, 290.3 MPa, and 266.2 MPa, due to porosity elimination as well as refinement of grains/particles [13].

Fig. 7 presents the fracture surfaces for the unprocessed base alloy and the as FS-processed tensile samples examined using SEM to determine their resulted failure pattern. Fig. 7(a), shows the as cast alloy tensile sample fracture surface. It can be seen that the surface was dominated by cleavage planes which indicate a brittle failure pattern; results in lower ductility. The cleavage pattern in fracture surface gives the indication of brittle material [9, 15]. This type of inter-granular failure fracture morphology is mostly caused by the coarse primary silicon. This is because, during tensile test higher amount of stress is transfer to the primary silicon crystals as a result of increased flow stress in the Al matrix. Thus, when the tensile stress surpasses the inherent primary silicon's fracture stress, the primary silicon cracked. The cracks instigated are extended alongside the interfaces between aluminum matrix and primary silicon crystals, afterward the neighboring cracks linkup and caused the materials to fracture [22]. After FSP, the FS-processed samples shows fracture surface with dimple rupture pattern Fig. 7(b-e). Formation of dimple pattern generally gives the indication of ductile material [6, 9]. FSP resulted in the refinement and redistribution of eutectic Si particles and breaking of continuous network of intermetallic phases. When these FSP samples were subjected to tensile testing the micro voids nucleated after certain level of straining, but interlinking of these micro

cracks became difficult and therefore allowed the ligament to deform considerably; resulted in high ductility. The nucleation of micro voids at the particle matrix interface represents dimple like pattern in the fracture surface [9], which is evident in Fig. 7(b-e).

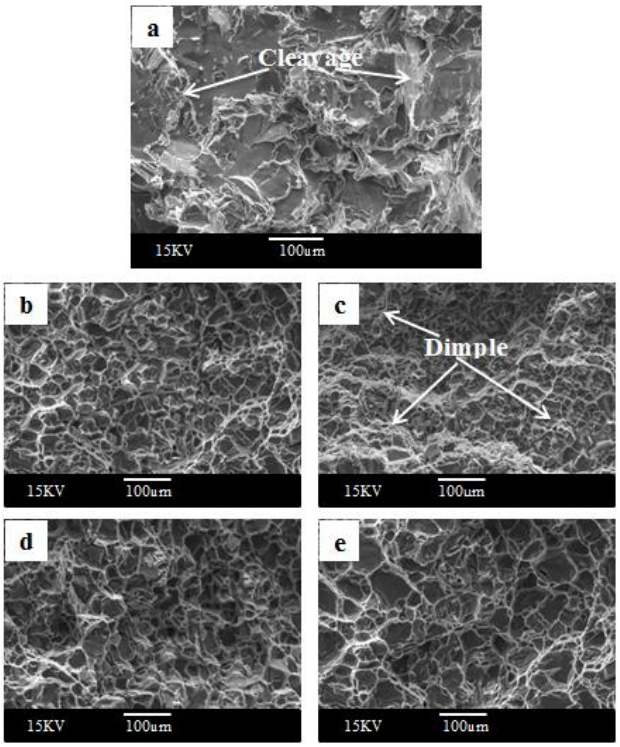

Fig. 7 The fracture surfaces of (a) cast base alloy, and as FS-processed tensile samples at 22 mm/min relative to (b) 800 rpm, (c) 1000 rpm, (d) 1200 rpm, and (e) 1400 rpm.

The as-cast LM28 alloy displayed mean hardness value of about 64.6 HV. Fig. 8 presents the variation of hardness of the stirred zone after FSP; sample processed at higher processing condition 1200 rpm and 1400 rpm their hardness profile appeared higher. However, it is appeared to be reduction in hardness within the SZ for samples processed at lower processing parameters 800 rpm and 1000 rpm. The reduction of hardness indicated softening of the processed material within the SZ during FSP. Such behaviour has often seen in heat treatable alloys, which tend to show reduction in hardness due to the coarsening and dissolution of precipitates strengthening during thermal cycle of the FSP/FSW [16]. Therefore the lower hardness values for the present investigation can be related to the breaking-up and dissolution of the intermetallic phases during thermal cycle of the FSP. The increase in hardness observed on the sample processed 1200/22, and 1400/22 condition, can be related to peak heat experienced by the sample at higher rotation rate which can lead to more intermetallic phases dispersed into the matrix and re-precipitate during cooling cycle of the sample. Similar result was reported by [4] in their work on AlSiCuNiMg alloy. The mean hardness was found increasing with raising the tool spindle rate.

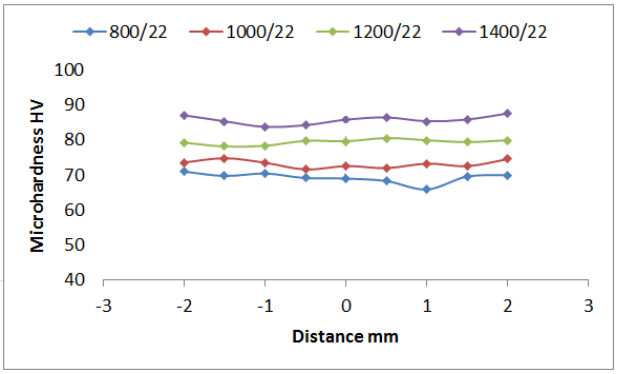

Fig. 8 Variation of mean hardness within the processed zone relative to tool rotation speed.

4. Summary

This work investigated the influence of FSP parameters on microstructure and tensile properties hypereutectic LM28 Al-Si alloy. The microstructure characteristics such as Si particles, formation of porosity had influence on tensile properties of base alloy. FSP shows significant effect on properties of the base metal, by refining the microstructure, and in turns, improve the tensile properties, by treating the casting defects such as porosity. Furthermore, both the coarse acicular silicon particles in the eutectic and primary silicon structures, together with the porosity were significantly reduced. FSP considerably lowered both the mean area sizes and the aspect ratio of the silicon, and porosity sizes. The as-cast LM28 alloy displayed Si particles mean area size, and aspect ratio around 155.1 μm² and 2.86 respectively. After FSP, the minimum silicon particle area and aspect ratio of size of 49.4 μm² and 1.63, were observed for sample FSP processed at 1000 rpm and 22 mm/min. All the tool speeds used influenced the tensile properties of the LM28 alloy significantly. Hardness of the processed zones shows improvement as the tool spindle speed increases. Higher hardness value was achieved at 1400 rpm tool speed, with the increase being around 32 %.

Acknowledgment

This paper was partly sponsored by the Center for Graduate Studies UTHM.

References

[1] Jayaraman, M., Sivasubramanian, R., and Balasubramanian, V. Effect of process parameters on tensile strength of friction stir welded cast LM6 aluminium alloy joints. *Journal of materials science and technology*, volume 25, (2009), pp. 655.

[2] Karthikeyan, L., Senthilkumar, V., and Padmanabhan, K. On the role of process variables in the friction stir processing of cast aluminum A319 alloy. *Journal of Materials and Design*, volume 31, (2010), pp. 761-771.

[3] Rao, A.G., Deshmukh, V.P., Prabhu. N., and Kashyap, B.P. Enhancing the machinability of

hypereutectic Al-30Si alloy by friction stir processing. *Journal of Manufacturing Processes*, volume 23, (2016), pp. 130-134.
[4] Tsai, F., and Kao, P. Improvement of mechanical properties of a cast Al–Si base alloy by friction stir processing. *Journal of Materials Letters*, volume 80, (2012), pp. 40-42.
[5] Mahmoud, T. Surface modification of A390 hypereutectic Al–Si cast alloys using friction stir processing. *Journal of Surface and Coatings Technology*, volume 228, (2013), pp. 209-220.
[6] Mahmoud, T., and Mohamed, S. Improvement of microstructural, mechanical and tribological characteristics of A413 cast Al alloys using friction stir processing. *Journal of Materials Science and Engineering: A*, volume 558, (2012), pp. 502-509.
[7] Alidokht, S.A., Abdollah-zadeh, A., Soleymani, S., Saeid, T., and Assadi, H. Evaluation of microstructure and wear behavior of friction stir processed cast aluminum alloy. *Journal of Materials Characterization*, volume 63, (2012), pp. 90-97.
[8] Chainarong, S., Muangjunburee, P., and Suthummanon, S. Friction Stir Processing of SSM356 Aluminium Alloy. *Journal of Procedia Engineering*, volume 97, (2014), pp. 732-740.
[9] Guru, P., S. Panigrahi, and Ram, G.J. Enhancing strength, ductility and machinability of a Al–Si cast alloy by friction stir processing. *Journal of Manufacturing Processes*, volume 18, (2015), pp. 67-74.
[10] Aktarer, S.M., Sekban, D.M., Saray, O., Kucukomeroglu, T., Ma, Z.Y., and Purcek, G. Effect of two-pass friction stir processing on the microstructure and mechanical properties of as-cast binary Al–12Si alloy. *Journal of Materials Science and Engineering: A*, volume 636, (2015), pp. 311-319.
[11] Karthikeyan, L., Senthilkumar, V.S., Balasubramanian, V., and Natarajan, S. Mechanical property and microstructural changes during friction stir processing of cast aluminum 2285 alloy. *Journal of Materials and Design*, volume 30, (2009), pp. 2237-2242.
[12] Ahmad, R., Abdulmalik, S.S., Usman, O.Y., and Danjuma, S.B. Microstructure and wear behavior of friction stir processed cast hypereutectic aluminum silicon. *in MATEC Web of Conferences*, volume 135, (2017), pp. 00048.
[13] Sun, N., and Apelian, D. Localized microstructure enhancement via Friction Stir Processing for die cast components. *Journal of La Metallurgia Italiana*, volume 10, (2013).
[14] Ma, Z., Sharma, S., and Mishra, R. Microstructural modification of as-cast Al-Si-Mg alloy by friction stir processing. *Journal of Metallurgical and Materials Transactions A*, volume 37, (2006), pp. 3323-3336.
[15] Rao, A.G., Deshmukh, V.P., Prabhu, N., and Kashyap, B.P. Ductilizing of a brittle as-cast hypereutectic Al–Si alloy by friction stir processing. *Journal of Materials Letters*, volume 159, (2015), pp. 417-419.
[16] Baruch, L.J, Raju, R., Balasubramanian, V., and Dinaharan, I. The effect of process parameters on the friction stir processed AS7U3G Aluminium Alloy. *Journal of Applied Mechanics and Materials*, volume 592, (2014), pp. 776.
[17] Ganesh, P. Finite element simulation in superplastic forming of friction stir welded aluminium alloy 6061-T6. *International Journal of Integrated Engineering*, volume 3, (2011), pp. 9-16.
[18] Tajiri, A., Uematsu, Y., Kakiuchi, T., Tozaki, Y., Suzuki, Y., and Afrinaldi, A. Effect of friction stir processing conditions on fatigue behavior and texture development in A356-T6 cast aluminum alloy. *International Journal of Fatigue*, volume 80, (2015), pp. 192-202.
[19] Miranda, R.M., Gandra, J.P., Vilaca, P., Quintino, L. and Santos, T.G. Surface Modification by Solid State Processing, *Woodhead Publishing Limited* (2013).
[20] Mohideen, S.R. and Zaidi, A.A. Influence of post weld heat treatment on the HAZ of low alloy steel weldments. *International Journal of Integrated Engineering*, volume 2, (2010).
[21] Ahmad, R. and Asmael, M.B.A. Influence of Lanthanum on Solidification, Microstructure, and Mechanical Properties of Eutectic Al-Si Piston Alloy. *Journal of Materials Engineering and Performance*, volume 25, (2016), pp.2799-2813.
[22] Li, Q., Xia, T., Lan, Y., Li, P., Fan, L. Effects of rare earth Er addition on microstructure and mechanical properties of hypereutectic Al–20% Si alloy. Journal of *Materials Science and Engineering: A*, volume 588, (2013), pp. 97-102.